Article

Modification of Fluorophore Photophysics through Peptide-Driven Self-Assembly

Kevin J. Channon, Glyn L. Devlin, Steven W. Magennis, Chris E. Finlayson, Anna K. Tickler, Carlos Silva, and Cait E. MacPhee

J. Am. Chem. Soc., **2008**, 130 (16), 5487-5491 • DOI: 10.1021/ja710310c • Publication Date (Web): 01 April 2008

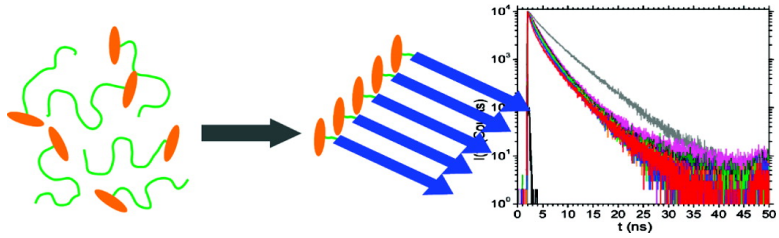

More About This Article

Additional resources and features associated with this article are available within the HTML version:

- Supporting Information
- Links to the 1 articles that cite this article, as of the time of this article download
- Access to high resolution figures
- Links to articles and content related to this article
- Copyright permission to reproduce figures and/or text from this article

View the Full Text HTML

J|A|C|S
ARTICLES

Published on Web 04/01/2008

Modification of Fluorophore Photophysics through Peptide-Driven Self-Assembly

Kevin J. Channon,[†] Glyn L. Devlin,[‡] Steven W. Magennis,[§] Chris E. Finlayson,[†] Anna K. Tickler,[†] Carlos Silva,[||] and Cait E. MacPhee*[,§]

Cavendish Laboratory, University of Cambridge, JJ Thomson Avenue, Cambridge, U.K., CB3 0HE, Department of Chemistry, University of Cambridge, Lensfield Road, Cambridge, U.K., CB2 1EW, SUPA, School of Physics, The University of Edinburgh, Mayfield Road, Edinburgh, U.K., EH9 3JZ, and Département de Physique, Université de Montréal, C. P. 6128 succ. centre-ville, Montréal, Québec, Canada, H3C 3J7

Received November 14, 2007; E-mail: cait.macphee@ed.ac.uk

Abstract: We describe the formation of self-assembling nanoscale fibrillar aggregates from a hybrid system comprising a short polypeptide conjugated to the fluorophore fluorene. The fibrils are typically unbranched, ~7 nm in diameter, and many microns in length. A range of techniques are used to demonstrate that the spectroscopic nature of the fluorophore is significantly altered in the fibrillar environment. Time-resolved fluorescence spectroscopy reveals changes in the guest fluorophore, consistent with energy migration and excimer formation within the fibrils. We thus demonstrate the use of self-assembling peptides to drive the assembly of a guest moiety, in which novel characteristics are observed as a consequence. We suggest that this method could be used to drive the assembly of a wide range of guests, offering the development of a variety of useful, smart nanomaterials that are able to self-assemble in a controllable and robust fashion.

Introduction

The emerging field of smart materials aims to design materials, at the molecular level, that exhibit specific combinations of physical and chemical functionality that may be inaccessible to traditional materials. Because of increased simplicity and flexibility of synthesis, supra-molecular self-assembly approaches for the production of functional materials are generating a great deal of attention.[1–3] Amyloid fibrils have attracted interest as nanomaterial scaffolds because of their potential for chemical and biological functionalization with nanometer precision.[4,5] Amyloid fibrils are large, highly ordered polypeptide aggregates which possess many desirable properties for nanomaterials engineering, such as high mechanical and chemical stability.[6–10] In the most part, this stability is derived from a β-sheet structural motif that is common to all amyloid fibrils. In this arrangement, individual peptides are connected through hydrogen bonds in a regular, continuous array, perpendicular to the fibril axis. This hydrogen-bonded array is thought to form consistently, with only a low sensitivity to the amino acid sequence.[11]

Here, we explore the utility of an amyloid-fibril-forming peptide in driving the assembly of a functional element—in this case, the polycyclic, aromatic fluorophore, fluorene. The self-assembly of functional systems represents a substantial challenge, because the molecular processes that drive the assembly can often be perturbed by the incorporation of the functional element. Indeed, previous independent studies have demonstrated that fluorene itself can drive the fibrillar assembly of short peptides via $\pi-\pi$ interactions between the fluorophores.[12–14] In this study, a fragment of the transthyretin protein ($TTR_{105–115}$) that is known to form especially well-ordered amyloid fibrils *in vitro*[6] was used as the protein component of the system. By choosing this well-characterized fiber-foming peptide, we aimed to retain the information for assembly exclusively within the peptide element without perturbing assembly significantly with inclusion of the guest molecule (Figure 1). Furthermore, in polymeric form, fluorene has displayed promising functionality as an organic electroluminescent material.[15,16] We thus anticipated that incorporation of the fluorophore into the nanoscale

[†] Cavendish Laboratory, University of Cambridge.
[‡] Department of Chemistry, University of Cambridge.
[§] SUPA, School of Physics, The University of Edinburgh.
[||] Département de Physique, Université de Montréal.

(1) Huie, J. C. *Smart Mater. Struct.* **2003**, *12*, 59816–59810.
(2) Sarikaya, M.; Tamerler, C.; Jen, A. K.-Y.; Schulten, K.; Baneyx, F. *Nat. Mater.* **2003**, *2*, 577–585.
(3) Whitesides, G. M.; Grzybowski, B. *Science* **2002**, *295*, 2418–2421.
(4) MacPhee, C. E.; Woolfson, D. N. *Curr. Opin. Solid State Mater. Sci.* **2004**, *8*, 141–149.
(5) Yeates, T.; Padilla, J. *Curr. Opin. Biotechnol.* **2002**, *12*, 464–470.
(6) Knowles, T. P. J.; Smith, J. F.; Craig, A.; Dobson, C. M.; Welland, M. E. *Phys. Rev. Lett.* **2006**, *96*, 238301.
(7) Kamatari, Y. O.; Yokoyama, S.; Tachibana, H.; Akasaka, K. J. *Mol. Biol.* **2005**, *349*, 916–921.
(8) Dirix, C.; Meersman, F.; MacPhee, C. E.; Dobson, C. M.; Heremans, K. J. *Mol. Biol.* **2005**, *347*, 903–909.
(9) Meersman, F.; Dobson, C. M. *Biochim. Biophys. Acta* **2006**, *1764*, 452–460.
(10) Dzwolak, W. *Biochim. Biophys. Acta* **2005**, *1764*, 470–480.
(11) Dobson, C. M. *Philos. Trans. R. Soc. London* **2000**, *356*, 133–145.
(12) Jayawarna, V.; Ali, M.; Jowitt, T. A.; Miller, A. F.; Saiani, A.; Gough, J. E.; Ulijn, R. V. *Adv. Mater.* **2006**, *18*, 611–614.
(13) Yang, Z.; Gu, H.; Fu, D.; Gao, P.; Kwok, J.; Xu, B. *Adv. Mater.* **2004**, *16*, 1440–1444.
(14) Zhang, Y.; Gu, H.; Yang, Z.; Xu, B. *J. Am. Chem. Soc.* **2003**, *125*, 13680–13681.

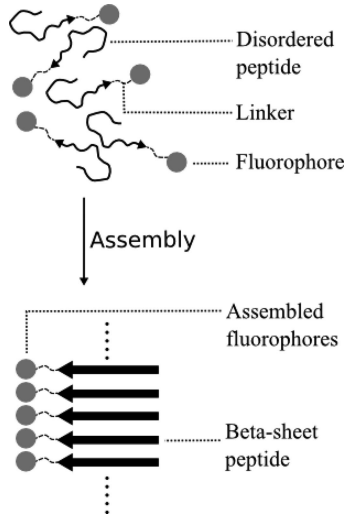

Figure 1. Schematic of the process of using the amyloid-fibril-forming properties of a peptide to assemble an attached guest group, a fluorophore in this case. The guest group is conjugated to the peptide prior to fibrilization (top), and the assembly of the peptide can be used to drive the assembly of the guest to form locally ordered structures (bottom).

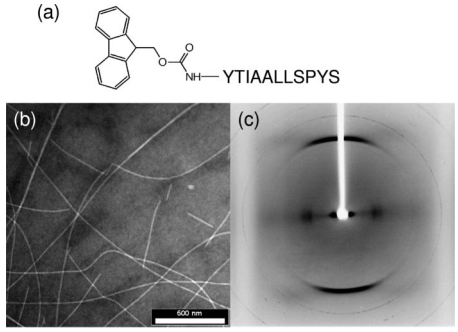

Figure 2. (a) Fmoc group shown conjugated to the amino acid sequence of $TTR_{105-115}$. (b) TEM image of F-TTR fibrils, scale bar indicates 500 nm. (c) Wide-angle X-ray fiber diffraction pattern of a partially aligned, dried stalk that was produced from a F-TTR gel.

scaffold of the amyloid fibril might elicit interesting photophysical responses.

Results

Fluorene was conjugated to the N-terminus of a peptide comprising amino acid residues 105−115 from the protein transthyretin (NH_2-Tyr-Thr-Ile-Ala-Ala-Leu-Leu-Ser-Pro-Tyr-Ser-CO_2H, $TTR_{105-115}$), F-TTR. Transmission electron microscopy (TEM) of samples from the F-TTR gel (Figure 2b) shows that it is composed of fibrillar species approximately 7 nm in diameter and some tens of microns long. Wide-angle X-ray fiber diffraction studies of partially aligned, dried stalks made from the gel (Materials and Methods) show meridional and equatorial reflections at 4.7 and ∼10 Å, respectively (Figure 2c). These reflections are consistent with β-sheets stacking along the fibril axis (∼10 Å) with a perpendicular orientation of the constituent β-strands (4.7 Å), typical of the common structural motif of amyloid fibrils.[17–19] Taken together, TEM and X-ray diffraction data confirm that the self-assembly process is driven primarily through amyloid formation, that is, via interpeptide contacts.

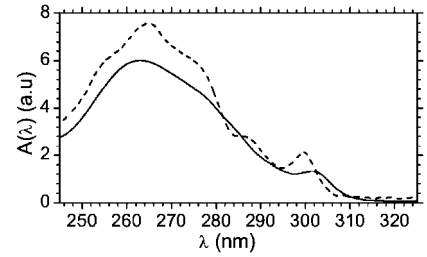

Figure 3. Electronic absorbance spectra of soluble (dashed trace) and fibrillar (solid trace) F-TTR in 20% methanol solution.

Having established that the β-sheet architecture of the amyloid fibrils is robust to the perturbing effects of the guest molecule, we subsequently investigated whether the assembly process induced any alteration to the properties of the fluorene moiety. As shown in Figure 3, there is a distinct change in the electronic absorbance spectrum of the fluorene moiety on fibrilization. In fibrillar F-TTR, there is a general redshift and broadening of the vibrational features that are evident in the soluble F-TTR peptide. The changes in absorbance described here are very similar to those observed by Nakano et al. in a novel dibenzofulvene polymer (pDBF) with pendant fluorene moieties.[20,21]

Nakano et al. were able to synthesize a number of small oligomers of pDBF and, in addition to absorbance spectroscopy, were able to examine the molecular structure by using high-resolution techniques, such as NMR spectroscopy. The atomic structure of pDBF indicates that the pendant fluorene groups are in a π-stacked geometry. The similarity in the absorbance spectra of pDBF and fibrillar F-TTR suggests that a similar effect occurs here. Large stretches of π-stacked fluorophores should, however, result in an X-ray reflection indicating the characteristic distance between them. The absence of this reflection suggests that regions of π-stacking are probably short, consisting of only a few fluorophores before the order is broken. The picture that emerges is thus one where there is not a continuous, unbroken array of fluorophores along the edge of the fiber but, rather, a series of smaller domains in which excitation is contained.

F-TTR was also examined for changes in its circular dichroism (CD) spectrum resulting from fibrilization. CD spectra of soluble and fibrillar F-TTR are shown in Figure 4. Fluorene is an achiral molecule and, as such, does not ordinarily display a CD spectrum, which is indeed found to be the case for soluble F-TTR (solid trace). This confirms that there is no direct, through-bond induction of chirality due to conjugation to the peptide. However, on fibrilization, a negative Cotton effect is clearly observed in the absorbance band of the fluorene moiety of F-TTR (dashed trace). The β-sheet structure of amyloid fibrils is ordinarily manifested in CD spectra as a minimum at ∼216 nm. However, this feature is not visible in this case because of the high absorbance of the fluorene moiety in this region. It is relatively common to observe the evolution of a CD spectrum because of interactions between achiral chro-

(15) Friend, R. H.; Gymer, R. W.; Holmes, A. B.; Burroughes, J. H.; Marks, R. N.; Taliani, C.; Bradley, D. D. C.; Dos Santos, D. A.; Brédas, J. L.; Lögdlund, M.; Salaneck, W. R. *Nature* **1999**, *397*, 121–128.
(16) Friend, R. H. *Pure Appl. Chem.* **2001**, *73*, 425–430.
(17) Blake, C.; Serpell, L. *Structure* **1996**, *4*, 989–998.
(18) Serpell, L.; Sunde, M.; Benson, M.; Tennent, G.; Pepys, M.; Fraser, P. *J. Mol. Biol.* **2000**, *300*, 1033–1039.
(19) Squires, A. M.; Devlin, G. L.; Gras, S. L.; Tickler, A. K.; MacPhee, C. E.; Dobson, C. M. *J. Am. Chem. Soc.* **2006**, *128*, 11738–11739.
(20) Nakano, T.; Yade, T. *J. Am. Chem. Soc.* **2003**, *125*, 15474–15484.
(21) Nakano, T.; Yade, T.; Fukuda, Y.; Yamaguchi, T.; Okumura, S. *Macromolecules* **2005**, *38*, 8140–8148.

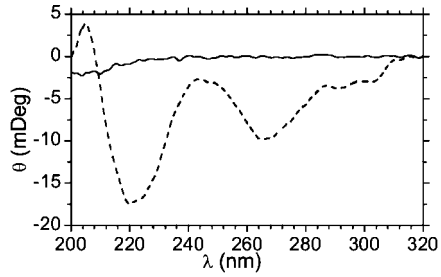

Figure 4. CD spectra of soluble (solid trace) and fibrillar (dashed trace) F-TTR in 20% methanol solution .

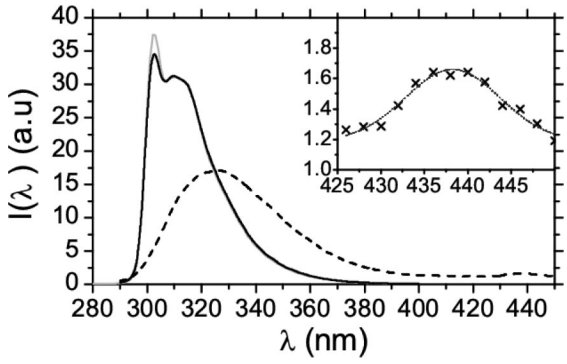

Figure 5. Steady-state emission spectra of soluble (solid trace, black) and fibrillar (dashed trace, black) F-TTR in 20% methanol aqueous solution. For comparison, emission from Fmoc-tyrosine is also shown (solid trace, light gray) in a 20% methanol aqueous solution. The inset shows in more detail the weak emission peak at 440 nm. Data is shown as crosses, a line is included to aid the reader's eye. $\lambda_{ex} = 265$ nm for all spectra.

mophores in chiral supra-molecular structures.[22] However, in these cases, a so-called split Cotton effect is observed, which is not the case here. We thus infer that the development of the Cotton effect in F-TTR is not likely to be the result of strong, chiral chromophore−chromophore interactions but a consequence of interactions of the fluorene moiety with the chiral amyloid fibril environment. Similar effects have been observed previously for fibrils produced by fluorene-conjugated dipeptides.[14]

In order to determine whether the nanoscale organization of the fluorene groups in the fibrils apparent from absorbance and CD spectroscopy elicited changes to the excited-state properties of the fluorophore, we examined F-TTR fibrils by using both steady-state and time-resolved fluorescence spectroscopy. Fluorescent emission from soluble F-TTR is virtually unchanged from fluorene alone; there is a well defined peak at approximately 302 nm, a second, broader peak at 310−315 nm, and no emission beyond 390 nm. On fibrilization, the sharp emission peak at 302 nm is not observed, and emission takes the form of a broad structureless peak with a single emission maximum in the region of 320−330 nm. Additionally, an extremely red-shifted emission peak at 440 nm is also observed (Figure 5, inset), which is indicative of excited-state dimer (excimer) emission. The excitation spectrum of the 440 nm emission peak was found to be virtually identical to the excitation spectrum of the main emission peak (data not shown), supporting the suggestion that the red-shifted peak is an excimer.[23]

The time dependence of F-TTR fluorescence was examined by using time-correlated single-photon-counting (TCSPC) spectroscopy (Figure 6). These studies reveal that soluble F-TTR has two dominant fluorescence decay components, with lifetimes of 5.6 ns (61%) and 3.0 ns (36%), and a third, minor, component with a lifetime of 0.7 ns (3%)—as measured in 20% methanol with $\lambda_{em} = 345$ nm. The fluorescence decays of Fmoc-Ser and Fmoc-Tyr were also measured ($\lambda_{em} = 305$ nm). These data can be fitted by two decay components. The major component of around 5.9 ns (63%) for Fmoc-Ser and 5.8 ns (65%) for Fmoc-Tyr has the same lifetime as the major component in soluble F-TTR. The minor component is longer at 10.4 ns (37%) and 10.6 ns (35%) for Fmoc-Ser and Fmoc-Tyr, respectively, and does not appear in the decay of F-TTR. Fmoc-Tyr, Fmoc-Ser, and F-TTR were also examined in neat methanol, and in each case, it was found that the emission displayed monoexponential kinetics with lifetimes of 6.0, 5.9, and 5.7 ns, respectively. We suggest that the multiple decay components observed in 20% methanol solutions may be due to dye−solvent interactions or some nonspecific aggregation phenomenon. It should be noted that no significant dependence of the dynamics on emission wavelength was observed with either Fmoc-Tyr, Fmoc-Ser, or soluble F-TTR (see Supporting Information).

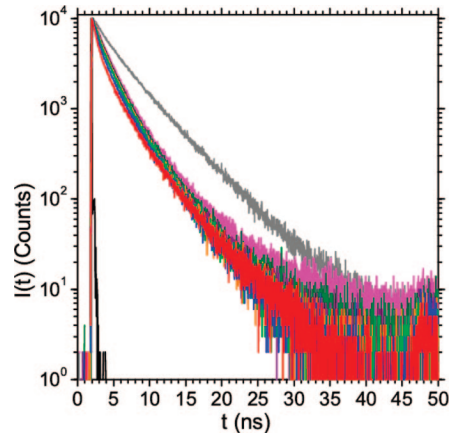

Figure 6. Time-resolved fluorescence of F-TTR. The emission of soluble F-TTR ($\lambda_{em} = 345$ nm) is shown in dark gray. The emission from fibrillar F-TTR at different emissive wavelengths is shown in red (310 nm), blue (320 nm), green (330 nm), orange (340 nm), purple (350 nm), dark green (360 nm), and pink (370 nm). The instrument response function is also shown in black. All samples are in 20% methanol solution.

When incorporated into the fibril structure, the lifetimes are similar to those found in soluble F-TTR, but their relative contributions are altered. For example, at an emission wavelength of 350 nm, the lifetimes are found to be 4.9, 2.4, and 0.97 ns, with fractional intensities of 23, 62, and 15%, respectively (no improvement to the fit was found by using a fourth component).The contribution of the shortest component is greatly increased in the fibril, and it was also found that as the detection wavelength is increased, there is a corresponding general increase in the lifetime of the excited state (see Supporting Information, Tables 1 and 2).Global analysis of the wavelength-dependent fluorescence decays, with lifetimes as common parameters, failed to produce a satisfactory fit by using three (or even four) decay components, indicating that there is a continuum of emissive states in the fibrils—as is commonly observed in fluorescent polymers. Full fitting parameters for all wavelengths are available in the Supporting Information. Overall, the steady-state and time-resolved fluorescence data

(22) Simonyi, M.; Bikadi, Z.; Zsila, R.; Deli, J. *Chirality* **2003**, *15*, 680–698.

(23) Lakowicz, J. *Principles of Fluorescence Spectroscopy*, 2nd ed.; Kluwer Academic and Plemum Publishers: New York, 1998.

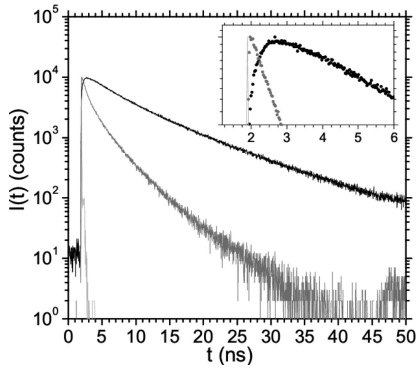

Figure 7. Time-resolved excimer fluorescence of F-TTR fibrils monitored at an emission wavelength of 330 nm (dark gray trace) and 440 nm (black trace). The instrument response function is also shown (light gray). The inset shows in more detail the risetime. All spectra were acquired in 20% methanol solution.

are indicative of exciton transfer within F-TTR fibrils from high-energy absorbance sites to low-energy trapping sites, from which significant emission occurs.

Time-resolved measurements also provide further evidence that the emission at 440 nm observed for F-TTR fibrils in steady-state spectra (Figure 5) is due to excimer emission. As shown in Figure 7, emission from F-TTR fibrils at this wavelength has a much longer fluorescence lifetime than that of soluble F-TTR. This is in clear contrast to the main emission peak of the fibrils (330 nm), which has a shorter lifetime than the soluble peptide. The fluorescence decay of this species is also well fitted by three components: two decaying components, with lifetimes of 5.0 ns (43%) and 12 ns (54%), and one risetime of 0.3 ns (3%). The presence of the risetime is notable, because it implies energy migration from high- to low-energy emissive site in fibrils.

In summary, we have demonstrated that an amyloidogenic peptide can drive the assembly of a small functional molecule (fluorene, in this case) with minimal perturbation to the amyloid fibril architecture and the induction of nanoscale organization of the functional element. Small, fluorene-conjugated peptides have also been observed to assemble into fibrillar structures in a number of previous, independent studies. However in these cases, the chemical characteristics of the fluorene moiety (specifically, $\pi-\pi$ interactions) were a determining feature of the systems' ability to self-assemble. Our aim in this work was to utilize fluorene only for its fluorescent functionality, retaining all information related to assembly within the peptide component. In this approach, the fluorene is intended to act as a passive cargo. We have found that the amyloid-like fibrils formed by $TTR_{105-115}$ are indeed robust to the addition of fluorene as a functional group. This apparent decoupling of function and assembly information within F-TTR leads us to infer that it should readily be possible to substitute the cargo for alternative groups, with functionalities suited to a wide range of tasks. This ability to rapidly arrive at self-assembled structures with diverse functions will obviously be important in the production of useful functional materials.

The peptide-driven, nanoscale organization of fluorene elicits interesting optical effects that could be of potential importance for functional materials. The induction of chirality in small functional groups decorating fibril scaffolds could, for example, be utilized to enable stereospecific catalysis. This function would be of great importance in the field of, for instance, drug design. Furthermore, the observation of exciton migration within the fibrils is notable given the importance of such processes in both optoelectronic and biological contexts—such as photovoltaics or photosynthesis.[24–26] In the case of photosynthesis, antenna complexes allow exciton transit to specific sites where charge separation can occur. By analogy, the incorporation of specific acceptor sites within a fibril system of the type discussed here could allow for interesting exciton trapping and light harvesting. These phenomena are the focus of ongoing studies within our laboratory.

Materials and Methods

Materials Preparation. $TTR_{105-115}$ was produced via solid-phase peptide synthesis. The final deprotection step was omitted, resulting in a fluorene attached to the $TTR_{105-115}$ peptide via a methoxycarbonyl linker, as in Figure 2a. Fibrils were formed by suspending F-TTR in neat methanol and by diluting to 40% methanol by using a pH 8.0, 10 mM potassium phosphate buffer with 120 mM sodium chloride, resulting in a final peptide concentration of 7 mM. The buffer solution was added at a temperature of 70 °C in order for the F-TTR to remain in solution. The solution was then held at 70 °C for approximately 2 min and allowed to cool to 40 °C at a rate of approximately 0.3 °C/min. The solution was left at 40 °C overnight; after this time, it appeared as a clear, viscous, gel-like solution.

Electron Microscopy. A 3 μL undiluted sample was deposited onto the carbon-coated FORMVAR film of a stainless steel 400-mesh TEM grid (Agar Scientific, UK). The grid was then rinsed with two 10 μL washes with ultrapure water ($\rho = 18$ MΩ cm^{-1}), each removed with filter paper, before being stained with 10 μL (1%, w/v) of uranyl acetate solution. Grids were allowed to air-dry before being stored. An FEI Tecnai 20 transmission electron microscope was used to study the grids. Images were acquired by using a CCD camera and analyzed by using Gimp (www.gimp.org) and ImageJ (http://rsb.info.nih.gov/ij) software packages.

X-ray Fiber Diffraction. A drop of the fibril gel was suspended between the wax-plugged ends of a pair of glass capillaries and allowed to dry. Before drying was complete, a second drop was added, then a third, and so forth. A total of four drops of fibril solution was added before the gel was allowed to completely dry overnight. The resulting fiber was translucent and showed good optical birefringence. Diffraction patterns were prepared and analyzed by using Fit2D (http://www.esrf.fr/computing/scientific/Fit2D) software.

Absorbance Spectroscopy. Absorbance spectra were acquired by using a Varian Cary 300-Bio UV−visible spectrophotometer, with 2 nm monochromator slit widths, 1 nm wavelength interval, 600 nm·min^{-1} scan rate, and 0.1 s integration time. Spectra shown are the mean of five spectra. Samples were prepared for steady-state spectroscopy by diluting the fibril gel into a 20% methanol solution at pH 8. The resulting data were prepared for publication by using OriginLabs software.

Fluorescence Spectroscopy. Steady-state fluorescence−excitation and emission spectra were acquired by using a Varian Cary Eclipse fluorescence spectrophotometer averaging 10 scans for each spectrum shown. Samples were prepared as for absorbance spectroscopy for steady-state spectroscopy by diluting the fibril gel 1000-fold into a 20% methanol solution at pH 8. The resulting data were prepared for publication by using OriginLabs software.

Time-resolved fluorescence measurements were made by TCSPC spectroscopy. The output of a femtosecond-laser system (10 W Verdi and Mira Ti-Sapphire laser, Coherent) was passed through a pulse picker (to reduce the repetition rate to 4.75 MHz), and the frequency was tripled to 270 nm. Fluorescence emission was

(24) Golbeck, J. H. *Biochim. Biophys. Acta* **1987**, *895*, 167–204.
(25) Glazer, A. N. *J. Biol. Chem.* **1989**, *264*, 1–4.
(26) van Grondelle, R.; Dekker, J. P.; Gillbro, T.; Sundstrom, V. *Biochim. Biophys. Acta* **1994**, *1187*, 1–65.

measured by using a spectrometer equipped with TCC900 photon counting electronics (Edinburgh Instruments), after passing through a 295 nm long-pass filter. The emission monochromator bandpass was 14 nm. The instrument response, measured with a Ludox scattering solution at the excitation wavelength, was ~50 ps full width at half-maximum. The counts in the peak channel were 10^4, and data were recorded with 2048 channels over a 50 ns range. Decay curves were analyzed by iterative reconvolution across the whole decay by using F900 software (Edinburgh Instruments). Global analyses were made by using FAST software (Alango). The data were fitted to a multi-exponential decay of the form:

$$\mathrm{I}(t) = A + \sum_{i=1}^{n} B_i \mathrm{e}^{-t/\tau_\mathrm{i}}$$

where τ_i is the lifetime, B_i is the amplitude of the ith decay component, and A is the background emission level. The quality of fits was determined by the reduced chi-squared parameter, χ^2, and visualization of residuals. No improvement in χ^2 was found by fitting with additional decay components. Negligible solvent fluorescence was found.

Circular Dichroism Spectroscopy. Spectra were acquired by using a Jasco J-180 spectropolarimeter at 20 °C in a quartz cuvette with a 10 mm path length. Samples of fibril gel were prepared for analysis by diluting 300-fold into a 20% methanol solution at pH 8. Spectra shown are the mean of five spectra.

Acknowledgment. We thank the Engineering and Physical Sciences Research Council of the United Kingdom for financial support. C.E.M. is a Royal Society University Research Fellow.

Supporting Information Available: Full fluorescence lifetime fitting parameters are available. This material is available free of charge via the Internet at http://pubs.acs.org.

JA710310C